AJNR

Gradient recalled echo MR imaging of the jugular foramen.

D L Daniels, L F Czervionke, P Pech, L E Hendrix, L P Mark, D F Smith, V M Haughton and A L Williams

AJNR Am J Neuroradiol 1988, 9 (4) 675-678
http://www.ajnr.org/content/9/4/675

Gradient Recalled Echo MR Imaging of the Jugular Foramen

David L. Daniels[1]
Leo F. Czervionke[1]
Peter Pech[2]
Lloyd E. Hendrix[1]
Leighton P. Mark[1]
David F. Smith[1]
Victor M. Haughton[1]
Alan L. Williams[1]

Axial T1-weighted spin-echo MR images have not proved to be effective in identifying normal structures in the jugular foramen. By correlating cryomicrotomic sections and axial T1-weighted gradient recalled echo images, we identified the neural and vascular contents of the jugular foramen. Further work with gradient recalled echo images is needed to determine the signal characteristics of jugular foraminal lesions.

Certain features of the MR appearance of the jugular foramen have been described. With a surface coil and T1-weighted spin-echo (SE) techniques, the jugular foramen can be demonstrated in parasagittal and semiaxial planes (i.e., nearly parallel to the endocranial opening of the foramen) [1]. However, with a head coil and axial T1-weighted SE images, we have found it very difficult to identify structures in the jugular foramen. Gradient recalled echo (GRE) images have proved useful in identifying cavernous venous spaces and cranial nerves [2]. In GRE images with flow compensation, vascular structures have high signal intensity designated "vascular enhancement." We believe axial head coil GRE images have the potential to demonstrate the contents of the jugular foramen and permit a side to side comparison of the jugular foramina.

Materials and Methods

Photographs of cryomicrotomic sections through the jugular foramina in three fresh, frozen cadaver heads were obtained by using a previously described technique [3]. The sectioning was in a plane parallel to the canthomeatal line.

Five normal volunteers and one patient with a glomus jugulare tumor (verified clinically and angiographically) were imaged on a 1.5-T GE Signa MR system with a head coil. Initially, quick sagittal T1-weighted SE images were used for localization. Subsequently, T1-weighted GRE axial images parallel to the canthomeatal line and from the pontomedullary junction to the foramen magnum, and parasagittal images through the jugular foramen were obtained. Technical factors for these GRE images included: 100/15/4 (TR/TE/excitations), flip angle of 90°, flow compensation, 256 × 256 matrix, field of view (FOV) of 20 cm, and 3-mm-thick contiguous sections. These factors were chosen on the basis of extensive work in a pilot study of MR imaging of the spine (Czervionke L., unpublished data). Also obtained in two volunteers and the patient were T1-weighted SE images with the following technical factors: 600/20/2 (TR/TE/excitations), 256 × 256 matrix, FOV of 20 cm, and 3-mm-thick contiguous axial images.

In the MR images and specimen photographs, cranial nerves IX–XI, the inferior petrosal sinus, the jugular bulb, and the internal carotid artery were identified by using published anatomic, CT, and MR literature [1, 4–8]

Results and Discussion

The jugular foramen consists of the pars nervosa (inferior petrosal sinus and cranial nerve IX [glossopharyngeal]) and, posteroinferolateral to it, the pars vas-

Received September 11, 1987; accepted after revision December 13, 1987.

This work was supported in part by NIH grant no. 1 RO1 AR 33667-01A2.

[1] Department of Radiology, Medical College of Wisconsin, Froedtert Memorial Lutheran Hospital, 9200 W. Wisconsin Ave., Milwaukee, WI 53326. Address reprint requests to D. L. Daniels.

[2] Department of Radiology, Uppsala University Hospital, S-751 85 Uppsala, Sweden.

AJNR 9:675–678, July/August 1988
0195–6108/88/0904–0675

cularis (jugular bulb and cranial nerves X [vagus] and XI [spinal accessory]). These two parts are separated by the jugular spine, which projects posteroinferomedially from the petrous bone (Fig. 1). The inferior petrosal sinus extends from the petrooccipital fissure through the pars nervosa to the jugular bulb [1, 4–8].

In progressively more inferior axial cryomicrotomic sections, the contents of the jugular foramen can be identified (Figs. 2 and 3). In the most superior sections, cranial nerve IX and, just medial to it, the inferior petrosal sinus in the pars nervosa are shown posteromedial to the petrous portion of the internal carotid artery. Cranial nerves X and XI are demonstrated in a common sheath near the anteromedial wall of the jugular bulb. In slightly more inferior sections, the jugular bulb forms an acute angle with the sigmoid sinus, where an osseous ridge projects inferiorly from the petrous bone. Within the jugular foramen, the jugular spine can be seen in cross section (Fig. 2).

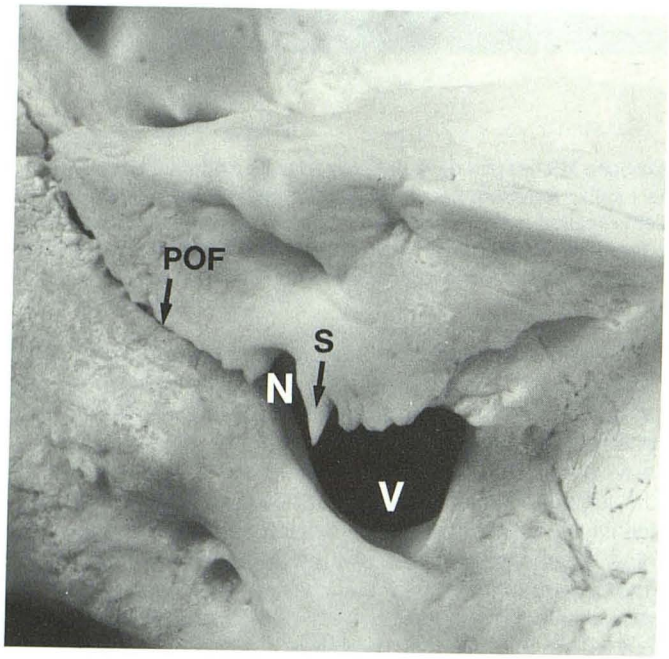

Fig. 1.—Jugular foramen in a dry skull shown from above and slightly posterolaterally. Note pars nervosa (N) and, slightly posteroinferolaterally, pars vascularis (V). Between them is the jugular spine (S) projecting posteroinferomedially. POF = petrooccipital fissure.

In progressively more inferior axial T1-weighted GRE images of normal volunteers, structures enhancing and isointense with the brainstem correlated with the vascular and neural contents, respectively, of the jugular foramen (Figs. 4 and 5). Cranial nerve IX was usually identified just lateral to the inferior petrosal sinus in the pars nervosa and posteromedial to the carotid artery, but was more difficult to visualize when the space between the artery and pars nervosa was very small. Cranial nerves X and XI together were consistently identified as appearing somewhat triangular or oval in shape just anteromedial to the jugular bulb. The jugular spine appeared as a small low-intensity area in the jugular foramen (Fig. 5). At the acute angle formed by the jugular bulb and sigmoid sinus, a spiral-shaped presumed flow artifact arose from the pointed edge of the petrous bone (Fig. 5). In two volunteers, T1-weighted SE images corresponding to the GRE images did not effectively demonstrate the jugular bulb and cranial nerves in the jugular foramen.

In parasagittal T1-weighted GRE images through the jugular foramen, cranial nerves X and XI were seen together extending anteroinferiorly just anterior to the jugular bulb in three of five volunteers (Fig. 6). Slightly more anteriorly and also extending anteroinferiorly, cranial nerve IX was shown only in one of these volunteers. Apparent low-intensity regions in the jugular vein just below the jugular bulb were attributable either to flow artifacts or partial volume averaging of adjacent structures.

In T1-weighted axial GRE images in a patient with a glomus jugulare tumor, the mass obliterated the contents of the ipsilateral jugular foramen (Fig. 7). The mass had a more

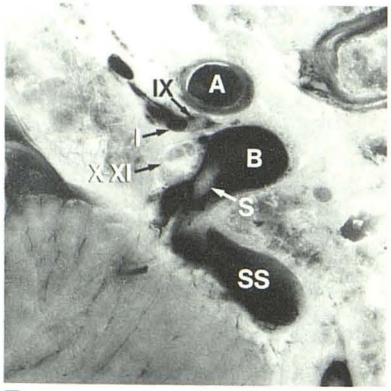

A B

Fig. 2.—*A* and *B*, Jugular foramina in axial cryomicrotomic sections at lower (*A*) and higher (*B*) magnification. Identified are cranial nerve IX just lateral to inferior petrosal sinus (I) in pars nervosa and posteromedial to petrous internal carotid artery (A) and cranial nerves X and XI just anteromedial to jugular bulb (B). In *B*, left jugular bulb is seen forming an acute angle with sigmoid sinus (SS). S = jugular spine.

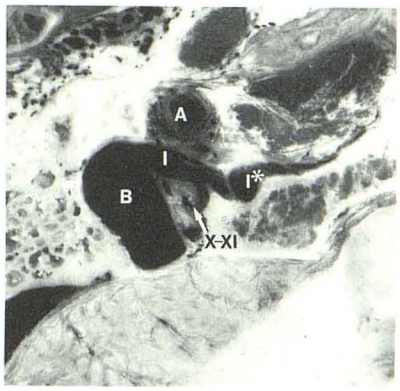

Fig. 3.—Jugular foramen in a slightly rotated axial cryomicrotomic section. Parts of inferior petrosal sinus, I and I*, are in pars nervosa and petrooccipital fissure, respectively. X-XI = cranial nerves X and XI, B = jugular bulb, A = internal carotid artery.

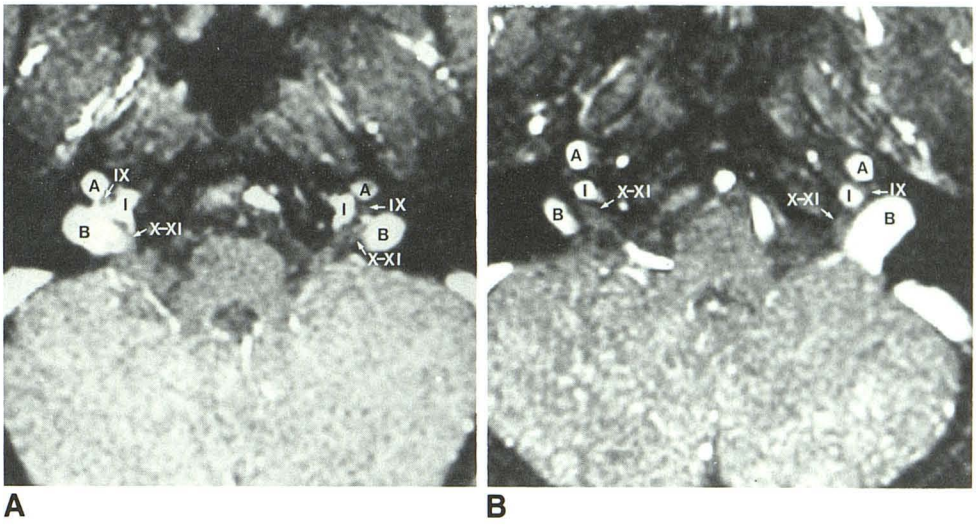

Fig. 4.—*A* and *B*, Jugular foramina in two volunteers in axial T1-weighted gradient recalled echo MR images. Cranial nerves IX (just lateral to inferior petrosal sinus [I] in pars nervosa) and X-XI (just anteromedial to jugular bulb [B]) are demonstrated. Petrous carotid artery (A) is seen anterolateral to pars nervosa. Note pronounced enhancement of vascular structures.

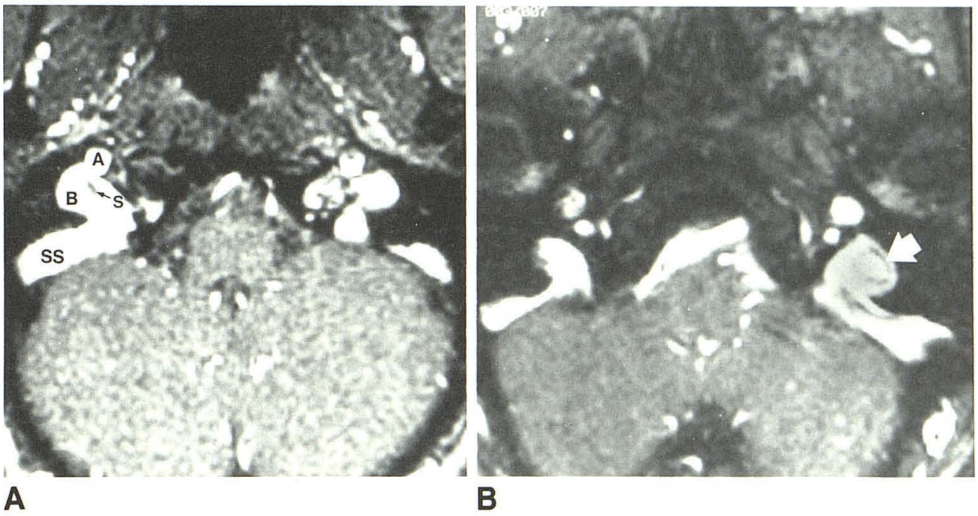

Fig. 5.—*A* and *B*, At a slightly lower level than that in Fig. 4, axial T1-weighted gradient recalled echo MR images in two volunteers. Jugular spine (S) and a presumed flow artifact (*arrow* in *B*) are identified in jugular foramina. A = petrous carotid artery, B = jugular bulb, SS = sigmoid sinus.

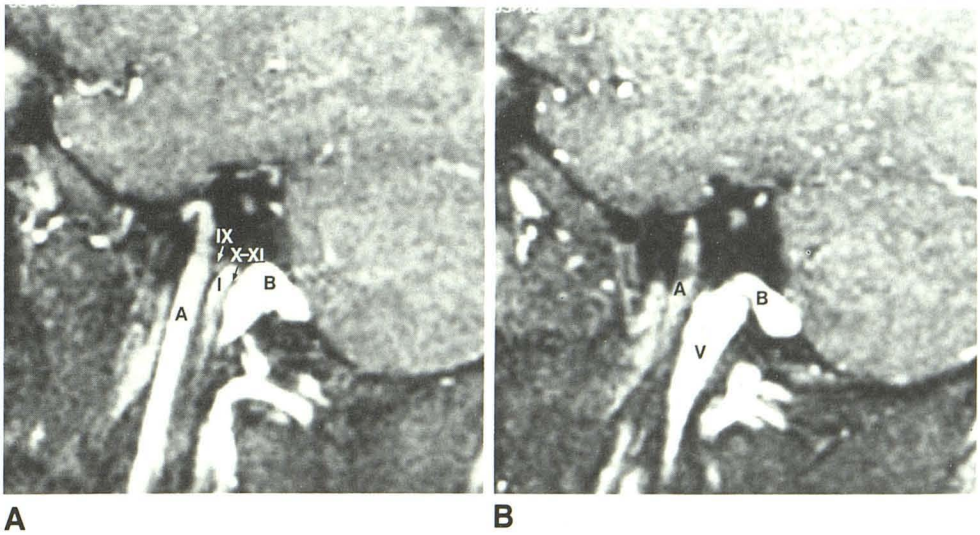

Fig. 6.—*A* and *B*, Jugular foramen in parasagittal T1-weighted gradient recalled echo MR images. In *A*, cranial nerves X-XI, anterior to jugular bulb (B), and IX, anterior to inferior petrosal sinus (I) in pars nervosa, are seen extending anteroinferiorly through skull base. Jugular vein (V) is shown in a slightly more lateral section (*B*). A = internal carotid artery.

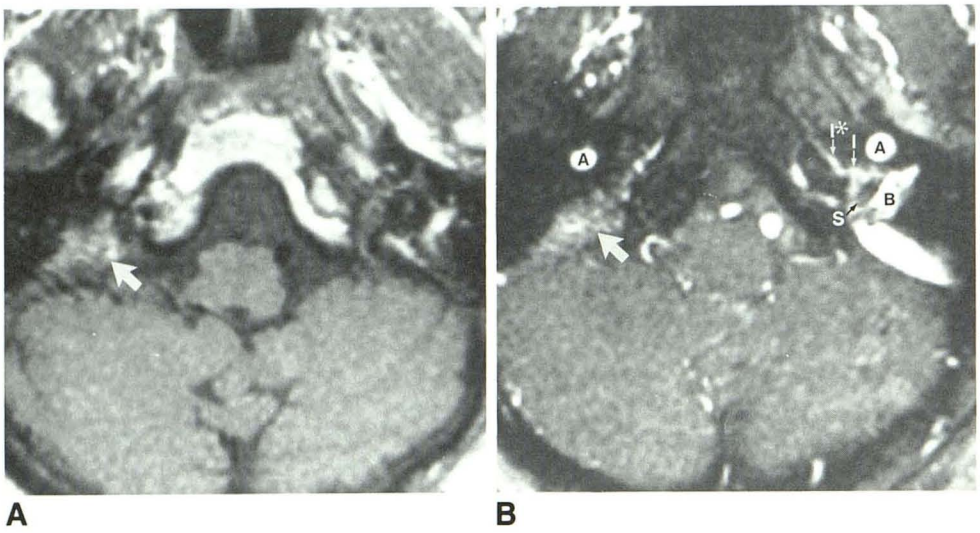

Fig. 7.—*A* and *B*, Glomus jugulare tumor (*arrow*) in axial T1-weighted SE (*A*) and gradient recalled echo (*B*) MR images. Tumor has a greater signal intensity than that of brainstem. A normal jugular foramen is shown on contralateral side in *B*. A = petrous internal carotid artery, B = jugular bulb, S = jugular spine, I = inferior petrosal sinus in pars nervosa, I* = inferior petrous sinus in petrooccipital fissure.

intense signal than that of the brainstem in both T1-weighted SE and GRE images, but in the latter the mass was less intense than that of the contralateral jugular bulb.

In conclusion, axial T1-weighted GRE images better demonstrate the normal contents of the jugular foramen than do SE images. Because cranial nerves in the jugular foramen can be identified, these GRE images should be able to exclude intraforaminal tumor. Further work with GRE images is needed to determine the signal characteristics of such tumors. A combination of parasagittal and axial T1-weighted SE and GRE images probably will be required to demonstrate the intraforaminal and extracranial extent of these tumors. The T1-weighted SE images sharply define the extracranial component because of the high signal intensity of adjacent fat, which is less intense in the GRE images.

REFERENCES

1. Daniels DL, Schenck JF, Foster T, et al. Magnetic resonance imaging of the jugular foramen. *AJNR* **1985**;6:699–703
2. Daniels DL, Czervionke LF, Bonneville JF, et al. MR of the cavernous sinus: value of spin echo and gradient recalled echo images. *AJNR* (in press)
3. Rauschning W, Bergstrom K, Pech P. Correlative craniospinal anatomy studies by computed tomography and cryomicrotomy. *J Comput Assist Tomogr* **1983**;7:9–13
4. Daniels DL, Williams AL, Haughton VM. Jugular foramen: anatomic and computed tomographic study. *AJNR* **1983**;4:1227–1232, *AJR* **1984**; 142:153–158
5. Lo WWM, Solti-Bohman LG. High-resolution CT of the jugular foramen: anatomy and vascular variants and anomalies. *Radiology* **1984**;150: 743–747
6. Gray H. *Anatomy of the human body*. Philadelphia: Lea & Febiger, **1966**
7. Rhoton AL, Buza RC. Microsurgical anatomy of the jugular foramen. In: Rand RW, ed. *Microneurosurgery*, 2nd ed. St. Louis: Mosby, **1978**: 252–264
8. Di Chiro G, Fisher RL, Nelson KB. The jugular foramen. *J Neurosurg* **1964**;21:447–460